IDENTIFYING VARIATIONS IN BASIN EJECTA THICKNESS USING LRO MINI-RF DATA. B. J. Thomson[1], D. B. J. Bussey[2], and J. T. S. Cahill[2], [1]Center for Remote Sensing, Boston University, Boston MA (bjt@bu.edu), [2]The Johns Hopkins University Applied Physics Lab, Laurel MD.

Introduction: Impact processes are among the most dominant forces that shape the lunar surface. The largest impacts – those that formed multi-ringed basins – occurred early in the Moon's history (prior to 3.8 Ga) [1]. Yet the effects of these basin-forming impacts are still evident on the surface today. Thompson et al. [2] used ground-based 70-cm synthetic aperature radar to infer the presence of South-Pole Aitken Basin ejecta on the southeastern nearside. Specifically, they observed a sharp gradient in the abundance of impact craters 1-16 km in diameter with radar-bright halos above and below the 48°S parallel between 5°W and 56°E lon. This difference was attributed to a transition from megaregolith that is inferred to be ~2.5 km thick in the south to ~1.5 km thick in the north, interpreted to be the result of South Pole Aitken (SPA) basin ejecta [2].

Here, we examine a global mosaic of Mini-RF S-band (12.6 cm) radar images to search for variations in the abundance of radar-bright craters that may be indicative of basin ejecta, particularly SPA. As SPA is located on the lunar far side, Mini-RF affords a view of a basin that is not attainable from a ground-based perspective.

Methods: Mini-RF is a dual-band, synthetic aperture radar (SAR) onboard LRO operating in the S-band (2.38 GHz, 12.6 cm wavelength) or X-band (7.14 GHz, 4.2 cm wavelength) [3]. In this work, we use S-band data processed into global mosaics [4], presented here at 64 pixels per degree (i.e., 473.8 m at the equator). Here we examined circular polarization ratio (CPR) data, which is defined as the ratio of the same sense (SC) circular polaritzation to opposite sense (OC) circular polarizations. Roughly 67% of the lunar surface was observed by Mini-RF S-band radar in monostatic polarimetric mode, including ~99% of both polar regions above 70°N and S latitude. Geolocation of surface features in the Mini-RF data is greatly aided by use of radar swaths that have been orthorectified to lunar topography [5].

Radar-bright crater background: Fresh impact craters on the Moon have distinctive optical, radar, and thermal properties relative to their surroundings [e.g., 6, 7-13]. Ejecta emplaced during the impact process are optically immature and therefore bright, resulting in a bright ring around a crater's rim that extends outward into filamentary rays [e.g., 6, 7-9]. A similar ring or "halo" of radar-bright material has been recognized in radar images of morphologically fresh craters [10-12], and it has been attributed to the rough textured, block-rich proximal ejecta. As stated in [12], bright radar signatures around craters typically imply enhanced populations of surface and/or subsurface rocks with sizes between 0.25 and 10 radar wavelengths, buried no deeper than 50 radar wavelengths. For Mini-RF 12.6 cm data, this implies an abundance of rocks >3 cm in diameter. Although not the focus of this study, many fresh to intermediate-aged impact craters also exhibit an outer halo of radar-dark material [14], a feature attributed to a block-poor zone of distal crater ejecta.

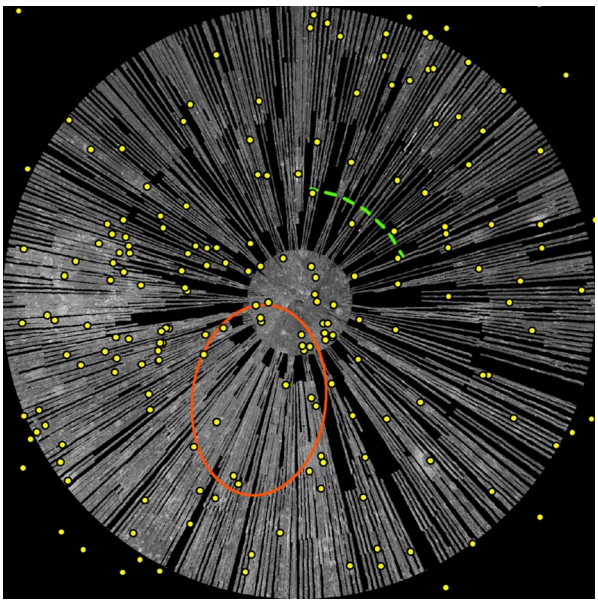

Figure 1. Mini-RF circular polarization ratio (CPR or μ_c) mosaic. View is polar stereographic projection centered at 90°S extending to the equator. SPA rim position is given with red ellipse [15]; inferred SPA ejecta boundary [1] is marked with green dashed line. Yellow circles mark locations of impact craters with radar-bright halos identified in this study.

Results: A south polar stereographic projection with the mapped distribution of radar-bright halos around impact structures is given in **Figure 1**. The topographic rim of the SPA basin (as defined by [15]) is marked with a yellow oval; the green line gives the SPA ejecta boundary inferred by [2]. Unlike with the 70-cm ground based radar data, there is no evident difference in the abundance of 1-16 km diameter radar-bright halo craters across this boundary. In addition, there is little apparent evidence for a similar boundary around other portions of the basin. Furthermore, alt-

hough the proximal ejecta of Orientale Basin has a distinctive radar signature [16], there is no such feature observed surrounding the rim of the much older SPA basin. The interior mare deposits within SPA exhibit a muted contrast with the surrounding highland terrain, which is significantly different from the marked highland-mare contrast evident with the nearside mare.

Discussion: Some of the differences between this present study and prior one may be partially attributable to differences in methodology. In their mapping of 70-cm radar bright craters [1], craters of intermediate to advanced age (i.e., those with radar-bright regions confined solely to regions inside of the crater rim) were included. However, such craters were excluded from our study: only radar-bright craters with bright exterior halos identified with 12.6 cm Mini-RF data were included in our mapped distribution.

Differences in methodology nonwithstanding, a lack of evident radial gradients in the abundance of 12.6 cm radar-bright craters around SPA may indicate that the presence or absence of basin ejecta does not strongly affect the presence or character of radar-bright halos at this wavelength. It was postulated by [1] that the thinner megaregolith (north of 48°S on the nearside) may have more abundant buried large (hundreds of meters in size) blocks that in turn provide for more consolidated crater ejecta that survives longer. Yet no evidence for such a difference in the target material block size abundance is readily apparent in the Mini-RF data.

Future work: We plan to continue our examination of radar-bight halos using full resolution Mini-RF swaths in order to better characterize the smaller-diameter population of craters. Differences in the abundance of radar-bright halos attributable to substrate properties may be more evident at smaller diameters.

References: [1] Spudis P.D. (1993) *The Geology of Multi-Ring Impact Basins*, 263 pp. [2] Thompson T.W. et al. (2009) *Geology*, *37*, 655-658. [3] Raney R.K. et al. (2011) *Proceedings of the IEEE*, *99*, 808-823. [4] Cahill J.T.S. et al. (2012) *LPSC*, *43*, abstract #2590. [5] Kirk R. et al. (2012) *LPSC*, *43*, abstract #2772. [6] Pieters C.M. et al. (1985) *JGR*, *90*, 12393-12413. [7] Grier J.A. et al. (2001) *JGR*, *106*, 32847-32862. [8] Hawke B.R. et al. (2004) *Icarus*, *170*, 1-16. [9] Werner S.C. & Medvedev S. (2010) *EPSL*, *295*, 147-158. [10] Thompson T.W. et al. (1974) *Moon*, *10*, 87-117. [11] Zisk S.H. et al. (1974) *Moon*, *10*, 17-50. [12] Thompson T.W. et al. (1981) *Icarus*, *46*, 201-225. [13] Bandfield J.L. et al. (2011) *JGR*, *116*. [14] Ghent R.R. et al. (2005) *JGR*, *110*, E02005. [15] Garrick-Bethell I. & Zuber M.T. (2009) *Icarus*, *204*, 399-408. [16] Cahill J.T.S. et al., in *LPSC*. (2011), vol. 42, pp. abstract #2134.